Eur J Nucl Med Mol Imaging
DOI 10.1007/s00259-010-1574-2

ORIGINAL ARTICLE

Type 1 cannabinoid receptor mapping with [^{18}F]MK-9470 PET in the rat brain after quinolinic acid lesion: a comparison to dopamine receptors and glucose metabolism

Cindy Casteels · Emili Martinez · Guy Bormans · Lluïsa Camon · Núria de Vera · Veerle Baekelandt · Anna M. Planas · Koen Van Laere

Received: 16 April 2010 / Accepted: 15 July 2010

Abstract
Purpose Several lines of evidence imply early alterations in metabolic, dopaminergic and endocannabinoid neurotransmission in Huntington's disease (HD). Using [^{18}F]MK-9470 and small animal PET, we investigated cerebral changes in type 1 cannabinoid (CB_1) receptor binding in the quinolinic acid (QA) rat model of HD in relation to glucose metabolism, dopamine D_2 receptor availability and amphetamine-induced turning behaviour.
Methods Twenty-one Wistar rats (11 QA and 10 shams) were investigated. Small animal PET acquisitions were conducted on a Focus 220 with approximately 18 MBq of [^{18}F]MK-9470, [^{18}F]FDG and [^{11}C]raclopride. Relative glucose metabolism and parametric CB_1 receptor and D_2 binding images were anatomically standardized to Paxinos space and analysed voxel-wise using Statistical Parametric Mapping (SPM2).
Results In the QA model, [^{18}F]MK-9470 uptake, glucose metabolism and D_2 receptor binding were reduced in the ipsilateral caudate-putamen by 7, 35 and 77%, respectively (all $p<2.10^{-5}$), while an increase for these markers was observed on the contralateral side (>5%, all $p<7.10^{-4}$). [^{18}F]MK-9470 binding was also increased in the cerebellum ($p=2.10^{-5}$), where it was inversely correlated to the number of ipsiversive turnings ($p=7.10^{-6}$), suggesting that CB_1 receptor upregulation in the cerebellum is related to a better functional outcome. Additionally, glucose metabolism was relatively increased in the contralateral hippocampus, thalamus and sensorimotor cortex ($p=1.10^{-6}$).
Conclusion These data point to in vivo changes in endocannabinoid transmission, specifically for CB_1 receptors in the QA model, with involvement of the caudate-putamen, but also distant regions of the motor circuitry, including the cerebellum. These data also indicate the occurrence of functional plasticity on metabolism, D_2 and CB_1 neurotransmission in the contralateral hemisphere.

Keywords Type 1 cannabinoid receptor · Small animal PET · QA · Huntington's disease · [^{18}F]MK-9470

C. Casteels · K. Van Laere
Division of Nuclear Medicine, KU Leuven and University Hospital Leuven,
Leuven, Belgium

C. Casteels · G. Bormans · K. Van Laere
MoSAIC, Molecular Small Animal Imaging Center, KU Leuven,
Leuven, Belgium

E. Martinez · L. Camon · N. de Vera · A. M. Planas
Institute for Biomedical Research (IIBB-CSIC), IDIBAPS,
Barcelona, Spain

G. Bormans
Laboratory for Radiopharmacy, KU Leuven,
Leuven, Belgium

V. Baekelandt
Laboratory for Neurobiology and Gene Therapy, KU Leuven,
Leuven, Belgium

C. Casteels (✉)
Division of Nuclear Medicine, University Hospital Gasthuisberg,
Herestraat 49 bus 7003,
3000 Leuven, Belgium
e-mail: cindy.casteels@med.kuleuven.be

Introduction

Huntington's disease (HD) is a devastating genetic neurodegenerative disorder, clinically characterized by involuntary movements, emotional disturbances and cognitive impairments. HD is caused by a CAG repeat expansion within exon 1 of the HD gene on chromosome 4 [1]. The mutated HD gene encodes an extended polyglutamine

Published online: 03 August 2010

stretch in the N-terminal domain of the huntingtin (htt) protein, which results in widespread neuronal degeneration preferentially within the striatum [2]. Despite the discovery of the genetic mutation associated with HD, the function of the abnormal gene product and the pathogenic mechanisms of the disease are still unknown.

Dysregulation of cannabinoid-mediated control of striatal function might play a critical role in the development of HD symptoms [3]. One of the earliest neurochemical alterations observed in HD patients is the loss of type 1 cannabinoid (CB_1) receptor binding in the basal ganglia, an alteration that significantly precedes the development of identifiable striatal neuropathology [4]. Likewise, CB_1 receptor mRNA levels were decreased in the absence of neuronal loss in the lateral striatum, cortex and hippocampus of transgenic mouse models of HD [5–9]. In the HD94 transgenic mice also decreases in the number of basal ganglia-specific binding sites and the activation of guanosine triphosphate (GTP)-binding proteins by CB_1 receptor agonists were noticed [5]. Loss of CB_1 receptors in the basal ganglia not only occurred in transgenic mice HD models, but also in rats after local intrastriatal application of 3-nitropropionic acid (3-NP), a toxin that reproduces the mitochondrial complex II deficiency characteristic of HD patients [10]. Delaying the onset of HD symptoms by enriched environments has been shown to selectively slow down the loss of CB_1 receptors in experimental HD [11].

In normal conditions, CB_1 receptors are abundantly distributed in different structures of the brain, controlling motor, cognition, emotional and sensory functions [12]. CB_1 receptors encompass together with a family of plant-derived, synthetic or endogenous compounds the endocannabinoid system (ECS). The ECS is a modulatory system that interacts with and regulates functioning of other neurotransmitter systems such as glutamate and γ-aminobutyric acid (GABA) [13].

So far, only in vitro and ex vivo data on the ECS exist in experimental HD. Studies of CB_1 receptor changes in experimental HD have focused on the basal ganglia, hippocampus and motor cortex, but have not assessed other brain regions [7, 9]. Also unknown is whether CB_1 receptor levels are changed in vivo. In vivo imaging of CB_1 receptors in the rat brain has recently become feasible due to the development of a CB_1-selective radioligand, [^{18}F]MK-9470 [14, 15].

A well-characterized and frequently used rat model of HD relies on the use of quinolinic acid (QA). QA is an endogenous metabolite in the brain that results in the degeneration of GABAergic striatonigral and striatopallidal projection neurons [16] with the relative [10] sparing of interneurons [17] after intrastriatal injection, a cellular pathology remarkably similar to that in patients with HD.

In this study, we have characterized the QA lesion rat model of HD in vivo with respect to CB_1 receptor binding using [^{18}F]MK-9470 and small animal positron emission tomography (PET) imaging. Also, dopamine D_2 receptor availability and glucose metabolism, all shown to be altered (early) in patients and animal models of HD [18, 19], were investigated in the same animals and correlated to the regional CB_1 receptor status.

Material and methods

Animals

Experiments were conducted on 21 female Wistar rats (Charles River, France) weighing 160–170 g at the start of the experiment. All animals were housed three to a cage, at an average room temperature of 22°C and a 12-h light/dark cycle. Food and water were given ad libitum. The research protocol was approved by the local Animal Ethics Committees of the Universities of Leuven and Barcelona and was according to European Ethics Committee guidelines (decree 86/609/EEC).

Striatal quinolinic lesion

All surgical procedures were performed under 1.5% halothane anaesthesia (4% during the induction period), at a rate of 1.5 ml/min. All rats were placed in a stereotactic head frame (David Kopf Instruments, Tujunga, CA, USA) [20], and a single unilateral hole was drilled in the skull over the left striatum using the bregma as reference. The neurotoxic and sham lesions in the left striatum were made by injecting 1 μl of QA (n=11, 240 nmol) or phosphate-buffered saline (PBS) (n=10, pH 7.4), respectively, at the following coordinates: anteroposterior +0.2 mm, lateral +2.8 mm and dorsoventral −4.5 mm [21]. The rate of infusion was 0.5 μl/min. After the injection, the needle was left in place for an additional 5 min before being slowly withdrawn from the brain.

Behavioural testing and weight

To assess toxin efficacy, the presence of QA-specific stereotypes was assessed in QA-lesioned rats after recovering using digital recording (Videotrack 2000, View Point, Lyon, France) [22]. Briefly, each animal (immediately after recovering from anaesthesia) was introduced into an individual cage (33.3×33.3 cm), in a soundproof room, and the behavioural activity was digitally recorded for a 3-h period. Digital records were analysed by a well-trained researcher evaluating the presence of QA-related stereotypes (head nodding, circling and rolling behaviour). All QA-treated rats

developed these stereotypes. Four weeks post-lesioning amphetamine-induced asymmetric rotational behaviour was monitored [23]. Amphetamine sulphate, supplied by the Ministry of Health of Spain, was injected intraperitoneally (i.p.) at a dose of 4 mg/kg free base. For each test, 5 min after amphetamine administration, the total number of complete turns clockwise and anticlockwise was counted over 30 min. The direction ipsilateral to the lesion is considered as positive. The analysis of amphetamine tests was based on net ipsilateral turns (defined as anticlockwise turning in cases of a left-sided injection). Additionally, changes in body weight were measured before lesioning, 24 h and 4 weeks after.

Radiotracer synthesis

CB_1 receptor imaging was performed in all animals (n=21) using the radioligand [^{18}F]MK-9470 (*N*-[2-(3-cyano-phenyl)-3-(4-(2-[^{18}F]fluorethoxy)phenyl)-1-methylpropyl]-2-(5-methyl-2-pyridyloxy)-2-methylproponamide), which is characterized by high specificity and high affinity for the CB_1 receptor (rat IC_{50} 0.9 nM) [14]. The precursor for tracer synthesis was obtained from Merck Research Labs (West Point, PA, USA) and labelling was performed using an [^{18}F]ethylbromide procedure as described previously [14]. The final product was obtained after high-performance liquid chromatography separation and had a radiochemical purity >95%. Specific activity was on average 219 GBq/μmol (specific activity range: 53–606 GBq/μmol). The tracer was administered in a sterile solution of 5 mM sodium acetate buffer pH 5.5 containing 6% of ethanol [24].

Functional images of the striatal dopamine system were obtained from each surviving rat using the D_2 receptor radioligand [^{11}C]raclopride (n=20) [25], while glucose metabolism was assessed using [^{18}F]FDG (n=20). [^{11}C] Raclopride was obtained by methylating the corresponding nor-precursor with [^{11}C]methyl triflate, whereas [^{18}F]FDG was prepared by using an Ion Beam Applications [^{18}F]FDG synthesis module. Approximately 18 MBq (500 μCi) of each radioligand (specific activity range: 53–760 GBq/μmol; injection volume: 500 μl) were injected into the tail vein using an infusion needle set.

Data acquisition

Small animal PET imaging was performed using a lutetium oxyorthosilicate detector-based tomograph (microPET Focus 220, Siemens Medical Solutions USA, Inc., Malvern, PA, USA), which has a transaxial resolution of 1.35 mm in full-width at half-maximum. Data were acquired in a 128×128×95 matrix with a pixel width of 0.475 mm and a slice thickness of 0.796 mm. The coincidence window width was set at 6 ns. Before imaging, the rats were anaesthetized with an i.p. injection of 50 mg of sodium pentobarbital (Nembutal, Ceva Sante Animale, Brussels, Belgium) per kilogram of body weight.

Imaging studies were performed on age-matched animals within 11–13 weeks post-lesioning for [^{18}F]MK-9470, 16–18 weeks post-lesioning for [^{18}F]FDG and 15–25 weeks post-lesioning for [^{11}C]raclopride. Dynamic 60-min [^{18}F]MK-9470 and [^{11}C]raclopride acquisitions were started immediately after tracer injection (frame duration: 4×15 s, 4×60 s, 5×180 s, 8×300 s), while [^{18}F]FDG measurements were obtained during 40 min starting 1 h after injection. Animals were scanned after overnight fasting for [^{18}F]MK-9470 and [^{18}F]FDG. The acquisition timing rationale and kinetics of the radioligands in rats have been described previously [24, 26].

Sinograms were reconstructed using filtered backprojection (FBP). No corrections were made for attenuation or scatter.

Small animal PET data processing and Statistical Parametric Mapping (SPM)

Parametric images based on standardized uptake values (SUV) [activity concentration (MBq/ml) × body mass(g)/injected dose (MBq)] were generated as a measure of absolute CB_1 receptor binding [14, 27]. No significant differences in body weight or injected activity were present between QA- and PBS-infused rats. We investigated absolute as well as relative uptake. Relative [^{18}F]MK-9470 uptake was expressed as SUV values normalized on whole-brain SUV. Parametric D_2 binding index (BI) images, representing D_2 receptor availability, were constructed by reference to the cerebellum using the Ichise multilinear reference tissue model 2 (MRTM2) module in PMOD [28]. Relative regional glucose metabolism was determined by count normalizing [^{18}F]FDG data to the whole-brain uptake. The within-subject test-retest variability of our imaging procedures is in a magnitude consistent with human data, i.e. <15% [15, 24, 29].

To obtain maximal use of image information without a priori knowledge, images were analysed on a voxel-by-voxel basis using SPM2. The procedure of spatial normalization and its validation have been described previously [24]. This methodology allows reporting results in coordinates directly corresponding to the Paxinos coordinate system for the rat brain.

SPM analysis was carried out using a categorical subject design (conditions: disease vs controls) on parametric [^{18}F]MK-9470 and [^{11}C]raclopride images, and on [^{18}F]FDG data of QA-lesioned rats. Spatially normalized images were masked to remove extracerebral signals that would disrupt the global normalization. All images were smoothed with an isotropic Gaussian kernel of 1.6 mm. For analysis of absolute [^{18}F]MK-9470 receptor binding, no proportional scaling was used and an analysis threshold of 0.8 of the mean

image intensity was applied. To study regional [^{18}F]MK-9470 uptake, proportional scaling was used. SPM analysis of absolute parametric D_2 binding data was performed without global normalization and with an absolute analysis threshold of –infinity (i.e. whole-brain analysis), while [^{18}F]FDG data were proportionally scaled with an analysis threshold of 80% to exclude white matter and ventricular activity.

To minimize false-positive findings, T-map data were interrogated at a peak level of $p<0.005$ (uncorrected) and extent threshold k_E >200 voxels (1.6 mm^3), as described previously [30]. Only those clusters that were significant at the $p<0.05$ (corrected) level were considered.

In addition, a voxel-based correlation analysis between relative [^{18}F]MK-9470 uptake/[^{18}F]FDG data and the following covariates was performed within the QA-lesioned group: (1) striatal [^{11}C]raclopride binding to characterize D_2 impairment and (2) the number of net ipsiversive turnings. A correlation analysis between relative [^{18}F]MK-9470 uptake and [^{18}F]FDG was carried out voxel-by-voxel wise using the BPM toolbox for SPM2 [31]. D_2 values were determined by a predefined volume of interest (VOI) analysis based on definition on the Paxinos atlas [24]. For D_2 impairment, the striatal affected to non-affected side BI ratio was obtained. D_2 impairment, FDG data and relative [^{18}F]MK-9470 uptake were expressed as percentage of normal values.

General statistics

Conventional statistics were carried out using STATISTICA v8.0 (StatSoft, Tulsa, OK, USA). Behavioural outcomes and body weight gain were analysed using unpaired *t* tests. Significance was defined at the 95% probability level. Data are mean ± SD.

Results

Subjects and behavioural data

PBS- and QA-infused rats showed the same pattern of body weight gain during the experiment (body weight gain after 24 h: −2±1 vs −14±2 g, $p<0.05$, and after 4 weeks: 62±20 vs 65±1 g, NS). No significant differences in the time of recovery from anaesthesia (5.6±1.8 vs 5.5±1.1 min) were found between PBS- and QA-infused rats. After surgery, QA-lesioned rats displayed, among others, head nodding, rolling and circling behaviour, with the net ipsiversive turnings after amphetamine administration significantly different from sham controls 4 weeks post-lesioning (151±23 vs 8±6, $p<0.05$).

SPM analysis

Absolute [^{18}F]MK-9470 binding values were not significantly different between QA-lesioned rats and control animals. Average cross-sectional small animal PET images of absolute [^{18}F]MK-9470 binding in controls and HD rats are shown in Fig. 1. As can be seen from this figure, the pattern of [^{18}F]MK-9470 uptake observed in the rat control brain is consistent with that previously reported ex vivo

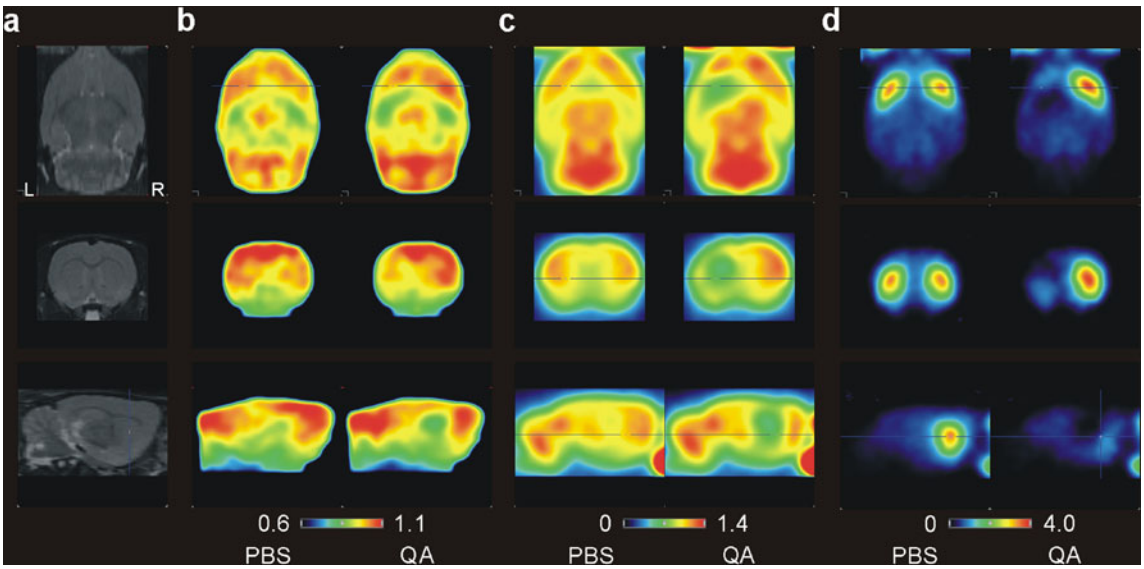

Fig. 1 Average cross-sectional small animal PET images, coregistered to MRI (**a**), of [^{18}F]MK-9470 binding (**b**), glucose metabolism (**c**) and [^{11}C]raclopride binding in the rat brain of sham-operated animals (*left*) and QA-lesioned rats (*right*). *Colour bars* indicate SUV values for [^{18}F]MK-9470, relative intensities for [^{18}F]FDG and binding indices for the dopamine D_2 receptor. Intersection points of 3 planes have been set to the mid-striatal level of the left hemisphere [i.e. (x, y, z)= (3.4, −0.2, −6.0, Paxinos coordinates)]. Images are oriented in neurological convention

[12], i.e. a fairly homogeneous and high uptake in the cortex, cerebellum and caudate-putamen.

When looking at regional changes by relative scaling to the global mean tracer binding, [^{18}F]MK-9470 values were decreased in the ipsilateral caudate-putamen by 7% ($p<2.10^{-5}$). Also, glucose metabolism and D_2 receptor binding were reduced in this region by 35 and 77%, respectively (all $p<2.10^{-11}$). An increase for each of these markers was observed on the contralateral side (>5%, all $p<7.10^{-4}$). The contralateral increase in relative metabolism

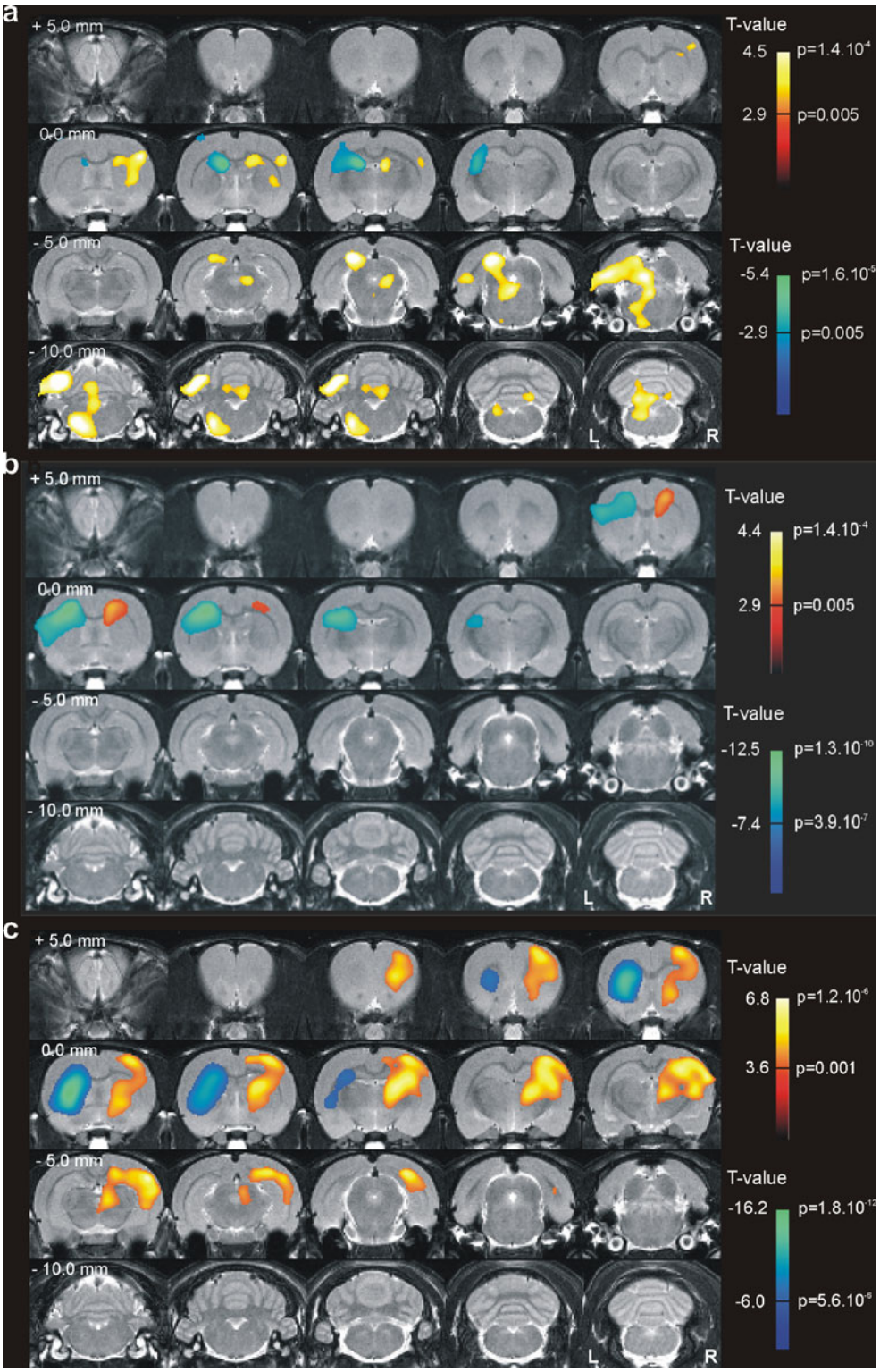

Fig. 2 Coronal brain sections showing overlays on the regions where a statistically significant increase (*red*) and decrease (*blue*) in relative [^{18}F]MK-9470 binding (**a**), D_2 receptor binding (**b**) and relative glucose metabolism (**c**) were observed in QA-lesioned rats (figure given at $p_{height}<0.005$ uncorrected) as compared to controls. Significance is shown with a T statistic colour scale, which corresponds to the level of significance at the voxel level. The distance between the sections is 1.00 mm with the position relative to the bregma (positive values for sections anterior to the bregma) on *top* of the sections in the *left column*. Images are oriented in neurological convention. The D_2 receptor deficit is located mainly in the anterior part of the caudate-putamen, which is in correspondence to the site of injection. The contralateral cluster of relative glucose metabolism encompasses the caudate-putamen, hippocampus, thalamus and sensorimotor cortex

extended towards the contralateral hippocampus, thalamus and sensorimotor cortex (+5.8±1.9%, $p=1.10^{-6}$).

Statistical parametric maps of [^{18}F]MK-9470, [^{11}C] raclopride and [^{18}F]FDG analysis are shown in Fig. 2. Average cross-sectional small animal PET images of glucose metabolism and [^{11}C]raclopride BI in controls and QA-lesioned rats are shown in Fig. 1.

Relative [^{18}F]MK-9470 binding was also increased in the cerebellum (+6.9±3.3%, $p=2.10^{-5}$), where it was inversely correlated to the number of ipsiversive turnings ($r=-0.94$, $p=7.10^{-6}$; Fig. 3a, b). No homologous regional correlations of [^{18}F]FDG and [^{11}C]raclopride with relative [^{18}F]MK-9470 uptake were observed. Relative [^{18}F]FDG values of the ipsilateral caudate-putamen were positively correlated with D_2 impairment ($r=0.92$, $p=9.10^{-5}$; Fig. 3c, d). Detailed cluster peak locations and p values of SPM analyses are shown in Table 1.

Discussion

Neurodegenerative diseases such as HD are characterized by gradually evolving selective neuronal death. Animal models using neurotoxins that produce similar patterns of neuronal degeneration may yield important information to elucidate its aetiology and may be used to assess neuroprotective/neuromodulatory approaches. In HD, much interest has recently been focused on the ECS as alterations in CB_1 receptor-mediated brain signalling might be related to hyperkinesia, typical of the earliest phase of the disease, or might be involved in the process of pathogenesis itself [32].

In this study, we have characterized CB_1 receptor alterations for the first time in vivo in QA-lesioned rats of HD using [^{18}F]MK-9470 and small animal PET. A whole-brain characterization of CB_1 receptors in this model is valuable and necessary prior to starting drug treatment [9].

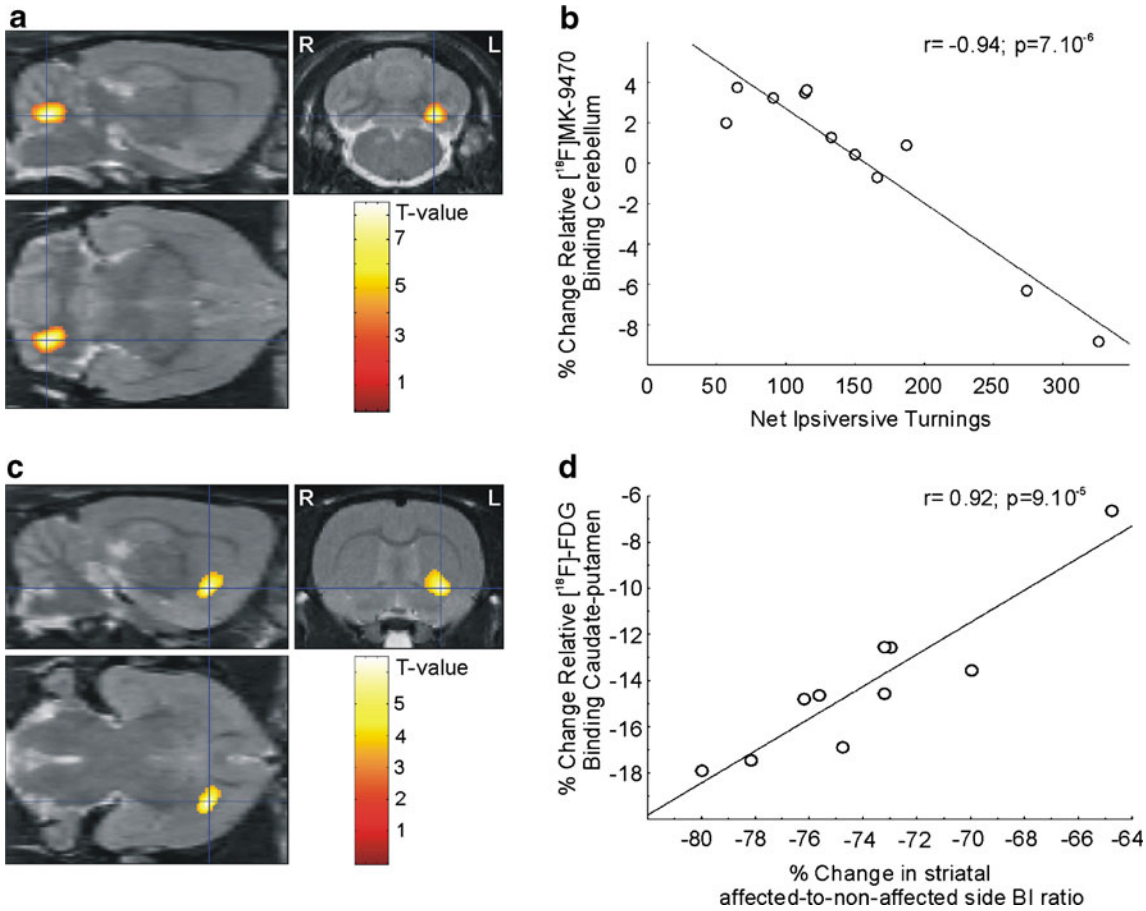

Fig. 3 **a**, **c** Coronal, transverse and sagittal brain sections with overlay of the cluster with decreased relative [^{18}F]MK-9470 binding (**a**) and decreased relative [^{18}F]FDG (**c**), expressed as percentage of controls, in relation to rotational behaviour (net ipsiversive turnings) and D_2 impairment for the QA group, respectively. Images are oriented in neurological convention. **b** Scatter plot of relative [^{18}F]MK-9470 uptake at the maximal peak location of the cerebellum in relation to ipsiversive turning behaviour of QA-lesioned rats. **d** Scatter plot of relative [^{18}F]FDG uptake at the maximal peak location of the lesioned caudate-putamen in relation to D_2 impairment of QA-lesioned rats, expressed as striatal affected to non-affected side BI ratio

Table 1 Peak locations for the clusters in the group comparison and correlation analysis (at $p_{height} \leq 0.005$ uncorrected, $k_E > 200$)

	Cluster level		Voxel level			Structure			Name
	p_{corr}	k_E	T	p_{uncorr}	Intensity difference (%)	x	y	z	
Categorical analysis: [^{18}F]MK-9470									
QA>PBS	<0.001	13498	6.82	<0.001	+6.9	4.2	−10.4	−4.0	Cerebellum
			5.56	<0.001		2.6	−7.2	−2.2	
			5.36	<0.001		0.2	−14.8	−6.2	
	<0.03	2048	4.45	<0.001	+5.1	−5.0	0.2	−3.2	Primary visual cortex and
			3.94	<0.001		−1.2	−2.0	−4.2	contralateral caudate-putamen
			3.74	≤0.001		−2.4	−0.6	−3.6	
QA<PBS	<0.01	2523	5.41	<0.001	−6.9	1.4	−1.4	−4.0	Ipsilateral caudate-putamen
			3.81	≤0.001		4.0	−2.8	−3.8	
			2.97	≤0.004		4.2	−0.4	−1.0	
Correlation analysis: negative correlation with net ipsiversive turnings									
	<0.03	311	8.48	<0.001	-	2.8	−12.4	−6.0	Cerebellum
Categorical analysis: [^{11}C]raclopride									
QA>PBS	≤0.002	1635	4.44	<0.001	+34.6	−2.2	0.4	−2.6	Contralateral caudate-putamen
QA<PBS	<0.001	56622	14.02	<0.001	−77.1	6.2	2.8	−9.6	Ipsilateral caudate-putamen
Categorical analysis: [^{18}F]FDG									
QA>PBS	<0.001	42077	6.78	<0.001	+5.8	−5.8	−4.8	−2.6	Association cortex
QA<PBS	<0.001	28854	16.17	<0.001	−35.1	3.2	0.2	−5.4	Ipsilateral caudate-putamen
Correlation analysis: positive correlation with D_2 impairment									
	<0.05	552	6.45	>0.001	-	3.2	0.0	−7.4	Ipsilateral caudate-putamen

Compared with sham controls, QA-infused rats showed an in vivo decrease in CB_1 receptor binding in the lesioned caudate-putamen. Reductions in CB_1 receptor levels of this region are in line with ex vivo samples of HD models at early and late stages of the disease. Lastres-Becker et al. demonstrated, in the absence of neuronal loss, a 30% reduction in the striatal CB_1 receptor density of HD94 transgenic mice using [^{3}H]CP55,940 autoradiography [5]. This reduction became more severe in 3-NP-treated rats when striatal degeneration was evident, presumably as a mere side effect caused by the progressive destruction of medium spiny GABAergic neurons [10]. We reported in the present study merely modest CB_1 receptor loss in the QA model, despite also evidence of prominent degeneration in these animals, as reflected by D_2 receptor imaging [33]. It appears from our findings as if CB_1 receptors try to restore basal levels, but remain insufficient as mentioned before. In the normal caudate-putamen, CB_1 receptors are expressed on presynaptic glutamatergic terminals originating in the cortex [34, 35]. In experimental and human HD, cortico-striatal glutamatergic transmission is severely impaired (for review see [36]), and QA lesions result in a secondary dying back of these terminals [37]. Relative upregulation of this CB_1 receptor population could conceivably represent a compensatory response, damping the excessive cortico-striatal glutamatergic drive that results from QA infusion [38] and reducing the excitotoxic mechanisms underlying HD [39]. However, within the caudate-putamen, CB_1 receptors are also expressed on striatal GABAergic interneurons that are labelled with parvalbumin and a few interneurons of the cholinergic population [40], from which their contribution to the observed effect cannot be excluded. Other contributing mechanisms may be changes in receptor affinity or in conformational state.

No correlation of this striatal CB_1 receptor deficiency with disease severity, measured by [^{18}F]FDG and [^{11}C]raclopride, was observed. In patients and animals with HD, metabolic abnormalities and reductions in dopamine binding are well described in striatal and extrastriatal regions, progressively decreasing upon symptom severity [18, 19, 41–45]. Here, [^{18}F]FDG values of the caudate-putamen were higher than, but positively correlated to D_2 impairment. Generally, [^{18}F]FDG uptake is a correlate of neuronal activity [46], but cellular metabolic decreases may also in part be compensated by [^{18}F]FDG uptake in reactive microglia, as has previously been shown in this model [47, 48].

Interestingly, in the current study, the unilateral QA lesion also causes CB_1 receptor-related abnormalities in the intact hemisphere, parallel to glucose metabolism and D_2 receptor binding. This observation suggests the occurrence of adaptive changes in the plasticity of the basal ganglia circuitry. Reactive compensation of the contralateral hemi-

sphere with regard to D_2/CB_1 receptors and glucose metabolism has not been demonstrated before in unilateral HD models by histology and imaging techniques. Previous animal experiments made use of between-hemisphere comparisons or only focused on the lesioned side in comparison to control data [19, 48]. Notably, studies with unilateral intranigral 6-hydroxydopamine (6-OHDA) application to model Parkinson's disease (PD) found similar findings of increased D_2 receptor densities in the contralateral caudate-putamen [49, 50]. There is also histologic evidence for interhemispheric projections from the striatum to the motor cortex [51], and upon lesioning, evidence of increased sprouting from intact to damaged hemispheres [52].

From our observations, it also appears as if reactive compensation is not limited to striatal structures only. In the QA model, we also found increased [^{18}F]MK-9470 tracer activity in the cerebellum, which inversely correlates to the number of ipsiversive turnings, suggesting that animals with the highest binding were related to a better functional outcome. In agreement with this finding, reduced CB_1 receptor levels in the cerebellum have been shown to be associated with locomotor hyperactivity in congenitally hypothyroid rats [53]. Motor hyperactivity is also a well-characterized feature observed in QA-treated animals, which appears already 2 weeks post-lesioning and lasts up to 6 months [54]. Here, the amphetamine-induced asymmetry test has been performed 4 weeks following the administration of QA intrastriatally, which is a time interval of 7–9 weeks from the [^{18}F]MK-9470 PET imaging. Putative alterations of the lesions occurring within that time interval are unlikely to have affected the behavioural outcome. It has clearly been shown that the lesions induced by QA result in stable ipsiversive turnings over time (range: 2–9 weeks) [55, 56]. Also, the striatal D_2 receptor asymmetry, underlying this behavioural effect, has been shown to reach a steady state, starting 16 days post-administration [19]. The striatal affected to non-affected side BI ratio of this study was also nearly constant among subjects between 15 and 25 weeks ($y = 0.0042x + 0.1875$).

In the design of this study, we have explicitly set the aim to investigate CB_1 receptor network alterations by using both absolute and relative [^{18}F]MK-9470 measurements. It is known that there is a higher physiologic interindividual variability of absolute regional [^{18}F]MK-9470 determinations in the human brain, in the order of several tens of per cent [14, 57]. Relative measurements have the advantage of being much more sensitive, allowing changes of 5–10% to be measured using SPM [58], as proven here.

Although QA neurotoxicity provokes loss of medium-sized spiny neurons in the injected striatal region, associated with motor hyperactivity [54] and spatial learning deficits [59], comparable to HD, it does not replicate the genetic hallmark underlying this disorder. This finding, together with the suggestion that (modest) species-specific differences exist in the brain CB_1 receptor distribution [14], reinforce the importance of translational research. Therefore, careful comparison to the human condition is needed to assess the in vivo validity and functional significance of our current findings, especially on the ECS which may open perspectives for neurochemical modulation of this currently untreatable neurodegenerative disorder.

In the present study, we have used QA rats because of the smaller brain size in transgenic mice which decreases sensitivity due to spatial resolution limits of small animal PET. In comparison to human studies, these QA rats received a relatively high dose of radiotracer. As the average weight of humans vs rats shows a ratio of approximately 300, care needs to be taken not to induce pharmacological effects. For the specific activity administered, the calculated % receptor occupancy of [^{11}C]raclopride was found to be in the range of 0.8–11%. This is still unlikely to induce a major pharmacological effect, such as dyskinesia, observed at an occupancy of over 50% for dopamine D_2 receptors. Also for [^{18}F]MK-9470, occupancies that are well below the pharmacological threshold were obtained (1–10 %) [60].

In conclusion, this in vivo study suggests modest regional changes in endocannabinoid transmission specific for CB_1 receptors in the QA rodent model of HD and points towards a compensatory role of the cerebellum. Our results additionally demonstrate the occurrence of functional plasticity in the QA lesion model on metabolism, D_2 and CB_1 neurotransmission, which implicates the need for carefulness when using the contralateral side as control condition.

Acknowledgements Merck & Co., Inc. is acknowledged for the availability of the [^{18}F]MK-9470 precursor, and for their critical revision of this manuscript and their improving suggestions. The authors thank Peter Vermaelen for his assistance in data acquisition, as well as the Leuven PET radiopharmacy team for tracer preparations. Financial support of the Research Council of the Katholieke Universiteit Leuven (OT/05/58), the Fund for Scientific Research, Flanders, Belgium (FWO/G.0548.06), the K.U. Leuven Molecular Small Animal Imaging Center (KUL EF/05/08), and the Institute for the Promotion of Innovation by Science and Technology in Flanders (SBO50151) is gratefully acknowledged. Part of this work is also performed under the European Commission FP6 project Diagnostic Molecular Imaging (DIMI), LSHB-CT-2005-512146.

Conflicts of interest None.

References

1. The Huntington's Disease Collaborative Research Group. A novel gene containing a trinucleotide repeat that is expanded and unstable on Huntington's disease chromosomes. The Huntington's Disease Collaborative Research Group. Cell 1993;72:971–83.
2. Vonsattel JP, Myers RH, Stevens TJ, Ferrante RJ, Bird ED, Richardson Jr EP. Neuropathological classification of Huntington's disease. J Neuropathol Exp Neurol 1985;44:559–77.

3. Fernández-Ruiz J. The endocannabinoid system as a target for the treatment of motor dysfunction. Br J Pharmacol 2009;156:1029–40.
4. Glass M, Dragunow M, Faull RL. The pattern of neurodegeneration in Huntington's disease: a comparative study of cannabinoid, dopamine, adenosine and GABA(A) receptor alterations in the human basal ganglia in Huntington's disease. Neuroscience 2000;97:505–19.
5. Lastres-Becker I, Berrendero F, Lucas JJ, Martín-Aparicio E, Yamamoto A, Ramos JA, et al. Loss of mRNA levels, binding and activation of GTP-binding proteins for cannabinoid CB1 receptors in the basal ganglia of a transgenic model of Huntington's disease. Brain Res 2002;929:236–42.
6. Naver B, Stub C, Møller M, Fenger K, Hansen AK, Hasholt L, et al. Molecular and behavioral analysis of the R6/1 Huntington's disease transgenic mouse. Neuroscience 2003;122:1049–57.
7. McCaw EA, Hu H, Gomez GT, Hebb AL, Kelly ME, Denovan-Wright EM. Structure, expression and regulation of the cannabinoid receptor gene (CB1) in Huntington's disease transgenic mice. Eur J Biochem 2004;271:4909–20.
8. Denovan-Wright EM, Robertson HA. Cannabinoid receptor messenger RNA levels decrease in a subset of neurons of the lateral striatum, cortex and hippocampus of transgenic Huntington's disease mice. Neuroscience 2000;98:705–13.
9. Dowie MJ, Bradshaw HB, Howard ML, Nicholson LF, Faull RL, Hannan AJ, et al. Altered CB1 receptor and endocannabinoid levels precede motor symptom onset in a transgenic mouse model of Huntington's disease. Neuroscience 2009;163:456–65.
10. Lastres-Becker I, Hansen HH, Berrendero F, De Miguel R, Pérez-Rosado A, Manzanares J, et al. Alleviation of motor hyperactivity and neurochemical deficits by endocannabinoid uptake inhibition in a rat model of Huntington's disease. Synapse 2002;44:23–35.
11. Glass M, van Dellen A, Blakemore C, Hannan AJ, Faull RL. Delayed onset of Huntington's disease in mice in an enriched environment correlates with delayed loss of cannabinoid CB1 receptors. Neuroscience 2004;123:207–12.
12. Herkenham M, Lynn AB, Little MD, Johnson MR, Melvin LS, de Costa BR, et al. Cannabinoid receptor localization in brain. Proc Natl Acad Sci U S A 1990;87:1932–6.
13. Katona I, Freund TF. Endocannabinoid signaling as a synaptic circuit breaker in neurological disease. Nat Med 2008;14:923–30.
14. Burns HD, Van Laere K, Sanabria-Bohórquez S, Hamill TG, Bormans G, Eng WS, et al. [18F]MK-9470, a positron emission tomography (PET) tracer for in vivo human PET brain imaging of the cannabinoid-1 receptor. Proc Natl Acad Sci U S A 2007;104:9800–5.
15. Casteels C, Lauwers E, Baitar A, Bormans G, Baekelandt V, Van Laere K. In vivo type 1 cannabinoid receptor mapping in the 6-hydroxydopamine lesion rat model of Parkinson's disease. Brain Res 2010;1316:153–62.
16. Beal MF, Kowall NW, Ellison DW, Mazurek MF, Swartz KJ, Martin JB. Replication of the neurochemical characteristics of Huntington's disease by quinolinic acid. Nature 1986;321:168–71.
17. Beal MF, Kowall NW, Swartz KJ, Ferrante RJ, Martin JB. Differential sparing of somatostatin-neuropeptide Y and cholinergic neurons following striatal excitotoxin lesions. Synapse 1989;3:38–47.
18. Antonini A, Leenders KL, Spiegel R, Meier D, Vontobel P, Weigell-Weber M, et al. Striatal glucose metabolism and dopamine D2 receptor binding in asymptomatic gene carriers and patients with Huntington's disease. Brain 1996;119(Pt 6):2085–95.
19. Araujo DM, Cherry SR, Tatsukawa KJ, Toyokuni T, Kornblum HI. Deficits in striatal dopamine D(2) receptors and energy metabolism detected by in vivo microPET imaging in a rat model of Huntington's disease. Exp Neurol 2000;166:287–97.
20. Vivó M, Camón L, de Vera N, Martínez E. Lesion of substantia nigra pars compacta by the GluR5 agonist ATPA. Brain Res 2002;955:104–14.
21. Paxinos G, Watson C. The rat brain in stereotaxic coordinates. San Diego: Academic; 1998.
22. Camón L, de Vera N, Martínez E. Polyamine metabolism and glutamate receptor agonists-mediated excitotoxicity in the rat brain. J Neurosci Res 2001;66:1101–11.
23. Visnyei K, Tatsukawa KJ, Erickson RI, Simonian S, Oknaian N, Carmichael ST, et al. Neural progenitor implantation restores metabolic deficits in the brain following striatal quinolinic acid lesion. Exp Neurol 2006;197:465–74.
24. Casteels C, Vermaelen P, Nuyts J, Van Der Linden A, Baekelandt V, Mortelmans L, et al. Construction and evaluation of multitracer small-animal PET probabilistic atlases for voxel-based functional mapping of the rat brain. J Nucl Med 2006;47:1858–66.
25. Farde L, Ito H, Swahn CG, Pike VW, Halldin C. Quantitative analyses of carbonyl-carbon-11-WAY-100635 binding to central 5-hydroxytryptamine-1A receptors in man. J Nucl Med 1998;39:1965–71.
26. Casteels C, Bormans G, Van Laere K. The effect of anaesthesia on [(18)F]MK-9470 binding to the type 1 cannabinoid receptor in the rat brain. Eur J Nucl Med Mol Imaging 2010;37:1164–73.
27. Terry GE, Liow JS, Zoghbi SS, Hirvonen J, Farris AG, Lerner A, et al. Quantitation of cannabinoid CB1 receptors in healthy human brain using positron emission tomography and an inverse agonist radioligand. Neuroimage 2009;48:362–70.
28. Ichise M, Liow JS, Lu JQ, Takano A, Model K, Toyama H, et al. Linearized reference tissue parametric imaging methods: application to [11C]DASB positron emission tomography studies of the serotonin transporter in human brain. J Cereb Blood Flow Metab 2003;23:1096–112.
29. Goffin K, Bormans G, Casteels C, Bosier B, Lambert DM, Grachev ID, et al. An in vivo [(18)F]MK-9470 microPET study of type 1 cannabinoid receptor binding in Wistar rats after chronic administration of valproate and levetiracetam. Neuropharmacology 2008;54:1103–6.
30. van Kuyck K, Casteels C, Vermaelen P, Bormans G, Nuttin B, Van Laere K. Motor- and food-related metabolic cerebral changes in the activity-based rat model for anorexia nervosa: a voxel-based microPET study. Neuroimage 2007;35:214–21.
31. Casanova R, Srikanth R, Baer A, Laurienti PJ, Burdette JH, Hayasaka S, et al. Biological parametric mapping: a statistical toolbox for multimodality brain image analysis. Neuroimage 2007;34:137–43.
32. Maccarrone M, Battista N, Centonze D. The endocannabinoid pathway in Huntington's disease: a comparison with other neurodegenerative diseases. Prog Neurobiol 2007;81:349–79.
33. Scherfler C, Scholz SW, Donnemiller E, Decristoforo C, Oberladstätter M, Stefanova N, et al. Evaluation of [123I] IBZM pinhole SPECT for the detection of striatal dopamine D2 receptor availability in rats. Neuroimage 2005;24:822–31.
34. Köfalvi A, Rodrigues RJ, Ledent C, Mackie K, Vizi ES, Cunha RA, et al. Involvement of cannabinoid receptors in the regulation of neurotransmitter release in the rodent striatum: a combined immunochemical and pharmacological analysis. J Neurosci 2005;25:2874–84.
35. Uchigashima M, Narushima M, Fukaya M, Katona I, Kano M, Watanabe M. Subcellular arrangement of molecules for 2-arachidonoyl-glycerol-mediated retrograde signaling and its physiological contribution to synaptic modulation in the striatum. J Neurosci 2007;27:3663–76.
36. Cepeda C, Wu N, André VM, Cummings DM, Levine MS. The corticostriatal pathway in Huntington's disease. Prog Neurobiol 2007;81:253–71.

37. Ellison DW, Beal MF, Mazurek MF, Malloy JR, Bird ED, Martin JB. Amino acid neurotransmitter abnormalities in Huntington's disease and the quinolinic acid animal model of Huntington's disease. Brain 1987;110(Pt 6):1657–73.
38. Pintor A, Tebano MT, Martire A, Grieco R, Galluzzo M, Scattoni ML, et al. The cannabinoid receptor agonist WIN 55,212-2 attenuates the effects induced by quinolinic acid in the rat striatum. Neuropharmacology 2006;51:1004–12.
39. Walker FO. Huntington's disease. Lancet 2007;369:218–28.
40. Fusco FR, Martorana A, Giampà C, De March Z, Farini D, D'Angelo V, et al. Immunolocalization of CB1 receptor in rat striatal neurons: a confocal microscopy study. Synapse 2004;53:159–67.
41. Ariano MA, Aronin N, Difiglia M, Tagle DA, Sibley DR, Leavitt BR, et al. Striatal neurochemical changes in transgenic models of Huntington's disease. J Neurosci Res 2002;68:716–29.
42. Wang X, Sarkar A, Cicchetti F, Yu M, Zhu A, Jokivarsi K, et al. Cerebral PET imaging and histological evidence of transglutaminase inhibitor cystamine induced neuroprotection in transgenic R6/2 mouse model of Huntington's disease. J Neurol Sci 2005;231:57–66.
43. Brownell AL, Chen YI, Yu M, Wang X, Dedeoglu A, Cicchetti F, et al. 3-Nitropropionic acid-induced neurotoxicity—assessed by ultra high resolution positron emission tomography with comparison to magnetic resonance spectroscopy. J Neurochem 2004;89:1206–14.
44. Ishiwata K, Ogi N, Hayakawa N, Oda K, Nagaoka T, Toyama H, et al. Adenosine A2A receptor imaging with [11C]KF18446 PET in the rat brain after quinolinic acid lesion: comparison with the dopamine receptor imaging. Ann Nucl Med 2002;16:467–75.
45. Kuwert T, Lange HW, Langen KJ, Herzog H, Aulich A, Feinendegen LE. Cortical and subcortical glucose consumption measured by PET in patients with Huntington's disease. Brain 1990;113(Pt 5):1405–23.
46. Jueptner M, Weiller C. Review: does measurement of regional cerebral blood flow reflect synaptic activity? Implications for PET and fMRI. Neuroimage 1995;2:148–56.
47. Dihné M, Block F, Korr H, Töpper R. Time course of glial proliferation and glial apoptosis following excitotoxic CNS injury. Brain Res 2001;902:178–89.
48. Moresco RM, Lavazza T, Belloli S, Lecchi M, Pezzola A, Todde S, et al. Quinolinic acid induced neurodegeneration in the striatum: a combined in vivo and in vitro analysis of receptor changes and microglia activation. Eur J Nucl Med Mol Imaging 2008;35:704–15.
49. Nikolaus S, Larisch R, Beu M, Forutan F, Vosberg H, Müller-Gärtner HW. Bilateral increase in striatal dopamine D2 receptor density in the 6-hydroxydopamine-lesioned rat: a serial in vivo investigation with small animal PET. Eur J Nucl Med Mol Imaging 2003;30:390–5.
50. Ferré S, Fuxe K. Dopamine denervation leads to an increase in the intramembrane interaction between adenosine A2 and dopamine D2 receptors in the neostriatum. Brain Res 1992;594:124–30.
51. Alloway KD, Smith JB, Beauchemin KJ, Olson ML. Bilateral projections from rat MI whisker cortex to the neostriatum, thalamus, and claustrum: forebrain circuits for modulating whisking behavior. J Comp Neurol 2009;515:548–64.
52. Pritzel M, Huston JP, Sarter M. Behavioral and neuronal reorganization after unilateral substantia nigra lesions: evidence for increased interhemispheric nigrostriatal projections. Neuroscience 1983;9:879–88.
53. Asúa T, Bilbao A, Gorriti MA, Lopez-Moreno JA, Del Mar Alvarez M, Navarro M, et al. Implication of the endocannabinoid system in the locomotor hyperactivity associated with congenital hypothyroidism. Endocrinology 2008;149:2657–66.
54. Scattoni ML, Valanzano A, Popoli P, Pezzola A, Reggio R, Calamandrei G. Progressive behavioural changes in the spatial open-field in the quinolinic acid rat model of Huntington's disease. Behav Brain Res 2004;152:375–83.
55. Song J, Lee ST, Kang W, Park JE, Chu K, Lee SE, et al. Human embryonic stem cell-derived neural precursor transplants attenuate apomorphine-induced rotational behavior in rats with unilateral quinolinic acid lesions. Neurosci Lett 2007;423:58–61.
56. Vazey EM, Chen K, Hughes SM, Connor B. Transplanted adult neural progenitor cells survive, differentiate and reduce motor function impairment in a rodent model of Huntington's disease. Exp Neurol 2006;199:384–96.
57. Barrero FJ, Ampuero I, Morales B, Vives F, de Dios Luna Del Castillo J, Hoenicka J, et al. Depression in Parkinson's disease is related to a genetic polymorphism of the cannabinoid receptor gene (CNR1). Pharmacogenomics J 2005;5:135–41.
58. Van Laere KJ, Versijpt J, Koole M, Vandenberghe S, Lahorte P, Lemahieu I, et al. Experimental performance assessment of SPM for SPECT neuroactivation studies using a subresolution sandwich phantom design. Neuroimage 2002;16:200–16.
59. Brasted PJ, Humby T, Dunnett SB, Robbins TW. Unilateral lesions of the dorsal striatum in rats disrupt responding in egocentric space. J Neurosci 1997;17:8919–26.
60. Kung MP, Kung HF. Mass effect of injected dose in small rodent imaging by SPECT and PET. Nucl Med Biol 2005;32:673–8.